Detailed study of NdFe2 and additional results relative to PrFe 2 and YbFe2. Comparison with other R.E. Fe2 compounds

C. Meyer, F. Hartmann-Boutron, Y. Gros, Y. Berthier, J.L. Buevoz

Classification
Physics Abstracts
76.80 — 75.50B — 75.50G

Detailed study of $NdFe_2$ and additional results relative to $PrFe_2$ and $YbFe_2$. Comparison with other R.E. Fe_2 compounds

C. Meyer, F. Hartmann-Boutron, Y. Gros, Y. Berthier

Laboratoire de Spectrométrie Physique (*), Université Scientifique et Médicale de Grenoble
B.P. 53 X, 38041 Grenoble Cedex, France

and J. L. Buevoz (**)

Institut Laue-Langevin, B.P. 156, 38042 Grenoble Cedex, France

(*Reçu le 30 juin 1980, révisé le 18 novembre, accepté le 23 décembre 1980*)

Résumé. — Cet article termine l'étude des trois composés phases de Laves $YbFe_2$, $NdFe_2$ et $PrFe_2$. Les propriétés de $NdFe_2$ y sont d'abord examinées de façon approfondie au moyen de nombreuses techniques (Rayons X, mesures d'aimantation, R.M.N. de ^{143}Nd, effet Mössbauer du ^{57}Fe, diffraction de neutrons). Quelques résultats additionnels concernant $PrFe_2$ et $YbFe_2$ sont également donnés. Enfin, les caractéristiques de ces trois composés sont comparées à celles du reste de la série, ce qui conduit aux conclusions suivantes : *a*) le champ cristallin sur la terre rare n'est pas constant dans la série, *b*) la partie isotrope du champ hyperfin sur le fer contient, d'une part, un terme de Lorentz et, d'autre part, des contributions transférées de spin et (probablement) d'orbite provenant des terres rares, *c*) la partie anisotrope de ce même champ n'est pas due aux seuls effets dipolaires et contient vraisemblablement, à la fois une contribution intrinsèque de la bande d et une contribution transférée due aux terres rares, *d*) le champ hyperfin vu par le noyau de terre rare est plus grand que le champ hyperfin de l'ion libre dans la deuxième moitié de la série et plus petit dans la première moitié, ces écarts étant probablement dus à la fois à des effets de self-polarisation et au champ hyperfin transféré venant des fers.

Abstract. — This paper concludes a study of the three Laves phase compounds $YbFe_2$, $NdFe_2$ and $PrFe_2$. The properties of $NdFe_2$ have been thoroughly investigated with a number of techniques including X-ray diffraction, magnetization measurements, ^{143}Nd N.M.R., ^{57}Fe Mössbauer effect and neutron diffraction. Some data is also reported on $PrFe_2$ and $YbFe_2$. The characteristics of these three compounds are compared with those of the rest of the RFe_2 series leading to the following conclusions : *a*) the crystalline field at the Rare Earth is not constant throughout the series, *b*) the isotropic part of the hyperfine field at the iron includes a Lorentz term together with spin and (probably) orbital transferred contributions arising from the R.E., *c*) the anisotropic part of the hyperfine field only partly results from dipolar effects and seems to involve both an intrinsic d band contribution and a transferred contribution from the R.E., *d*) the hyperfine field at the Rare Earth nucleus is higher than the free ion hyperfine field in the second half of the series and lower in the first half of the series these deviations probably resulting from both self polarization effects and transferred fields from the iron.

1. **Introduction.** — During the past twenty years, the cubic Rare Earth (R.E.) Iron Laves phase compounds, RFe_2, have been the subject of extensive investigations. However these studies have mainly dealt with compounds belonging to the second half of the Rare Earth series (Gd ... Tm, Lu). In the first half the only compounds then available were $CeFe_2$, in which Ce is tetravalent, and $SmFe_2$, which is also not representative, because of the *J-J* mixing in the Sm^{3+} ion. In the second half, $YbFe_2$ had not been prepared.

By using high pressures and temperatures (80 kbars, 1 200 °C) we have succeeded in preparing the three compounds $YbFe_2$, $NdFe_2$ and $PrFe_2$, whose existence was first reported by Cannon *et al.* [1]. The Mössbauer (^{57}Fe, ^{170}Yb) and magnetization studies of $YbFe_2$ have been reported in great detail in references [2-7] while some preliminary results concerning $NdFe_2$ and $PrFe_2$ are presented in references [4, 5, 6]. This paper is mainly devoted to the properties of $NdFe_2$;

(*) Laboratoire associé au C.N.R.S. (L.A. n° 8).
(**) Now at C.N.E.T., 4, Chemin des Prés, 38240 Meylan.

however in addition some data on $PrFe_2$ and $YbFe_2$ are also included. Finally the results obtained on these three compounds are compared with the previous work on the RFe_2 series and some general conclusions are drawn. Note that both $NdFe_2$ and $PrFe_2$ have also been prepared recently by Shimotomai *et al.* [8, 9].

Before introducing the new compounds it may be useful to briefly recall the main features of the RFe_2 compounds.

2. **Main features of the RFe_2 compounds [10]. Organization of the paper.** — 2.1 EXCHANGE INTERACTION. — It is well known that the exchange interactions in the RFe_2 are dominated by the ferromagnetic Fe-Fe coupling, which is responsible for the high Curie temperatures of these materials ($\sim$ 600 K). Second in magnitude is the iron-rare earth coupling which is generally written in the form :

$$\mathcal{H}_{ex} = -2\,\mathcal{J}_{ex}\,\mathbf{S}_{Fe}.\mathbf{S}_{R.E.} = -2(g_J - 1)\,\mathcal{J}_{ex}\,\mathbf{S}_{Fe}.\mathbf{J}_{R.E.} \tag{1}$$

with $\mathcal{J}_{ex}$ negative and approximately constant throughout the series. This coupling, of the order of 100 K, accounts for the variation of the Curie temperature between, roughly, 600 and 800 K. Finally the R.E.-R.E. coupling is small ($\sim$ 10-30 K) and is usually neglected.

The compounds of the second half of the series, for which $(g_J - 1) > 0$ are all ferrimagnetic, including $YbFe_2$. Consequently, in the first half, for which $(g_J - 1) < 0$, ferromagnetism is expected. Since $SmFe_2$ is atypical because of the peculiarities of the Sm^{3+} ion, the investigation of $NdFe_2$ and $PrFe_2$ is interesting in this respect.

2.2 MAGNETIZATION DIRECTION AND MAGNETOCRYSTALLINE ANISOTROPY. — In the RFe_2 the R.E. occupy cubic sites (8*a*) and the irons occupy trigonal sites (16*d*). The iron sites are not magnetically equivalent. The hyperfine structure of the iron is anisotropic (see next section), which means that the ^{57}Fe Mössbauer spectra are therefore split into subspectra whose aspect is characteristic of the direction of the magnetization **M**, which is itself determined by the magnetocrystalline anisotropy.

The anisotropy of the iron is small ($\sim$ 1 K per formula unit). In contrast, with the exception of YFe_2, $GdFe_2$ and $LuFe_2$, the cubic anisotropy of the R.E., associated with crystal field effects, is large and determines the direction of the easy axis of **M**.

2.3 HYPERFINE INTERACTIONS AT THE IRON. — Each iron site has trigonal symmetry around one of the $\langle 111 \rangle$ directions. An electric field gradient with axial symmetry around this same direction exists at the iron nucleus, with

$$e^2 qQ/2 \sim -0.5 \text{ mm/s}$$

in all members of the series. The iron nucleus also sees a hyperfine field,

$$\mathbf{H}_t = \mathbf{H}_n + \mathbf{H}_d \tag{2}$$

consisting of an isotropic part $\mathbf{H}_n$ (opposing the iron moment $\boldsymbol{\mu}_{Fe}$) and of an anisotropic part :

$$\mathbf{H}_d = \mathbf{A}_d \frac{\boldsymbol{\mu}_{Fe}}{|\mu_{Fe}|} \tag{2'}$$

which was originally identified with the dipolar field $\mathbf{H}_{dip}$ created at an iron atom by the magnetic moments of its neighbours within a Lorentz sphere (see Appendix). The tensor $\mathbf{A}_d$ for the four types of iron sites is given by equation (B.4) of Appendix II of reference [3]. As an example, for the site 5/8, 5/8, 5/8, associated with $(1/\sqrt{3}, 1/\sqrt{3}, 1/\sqrt{3})$:

$$\mathbf{A}_d = \begin{pmatrix} 0 & A_d & A_d \\ A_d & 0 & A_d \\ A_d & A_d & 0 \end{pmatrix}. \tag{3}$$

If $\mathbf{A}_d$ is of dipolar origin, then the parameter A_d is equal to [2] :

$$A_d = A_{dip} = a_0^{-3}[40.8\sqrt{2}\,|\,\mu_{Fe}\,| \mp 19.5\sqrt{2}\,|\,\mu_{R.E.}\,|] \tag{4}$$

where the second term is negative for the first half and positive for the second half of the R.E. series. However there is a discrepancy between the computed dipolar value, A_{dip}, and the experimental value, A, of A_d. In the second half of the RFe_2, A is often 20-40 % larger than A_{dip} and, for $SmFe_2$: $A \sim 6\,A_{dip}$. Some authors [11] have attributed this discrepancy to an enhancement of the dipolar field by the conduction electrons. As we will see below, such an explanation cannot be correct for $NdFe_2$ in which the computed parameter is nearly zero, but where the experimental value, A, is very large. An important part of the present paper will be devoted to this problem of the h.f.s. anisotropy at the iron.

2.4 ORGANIZATION OF THE PAPER. — For each material we will first describe the preparation and report on the purity, the Curie temperature and the magnetization curves. The magnetization measurements are important because the computed dipolar parameter A_{dip} evidently depends on the magnetic structure, and anomalous experimental values of A might result from an unusual magnetic structure.

The following paragraphs will describe the Mössbauer study, with and without an applied magnetic field, and, in the case of $NdFe_2$, complementary measurements using other techniques including neutron diffraction and N.M.R.

Finally the properties of $NdFe_2$, $PrFe_2$, $YbFe_2$ will be compared with those of the other RFe_2.

3. **Study of $NdFe_2$.** — 3.1 PREPARATION, CURIE TEMPERATURE, AND MAGNETIZATION CURVES. — 3.1.1 *Preparation and identification.* — The preparation of $NdFe_2$ is identical to that of $YbFe_2$, described in [2], except that we started with an equiatomic mixture of Nd and Fe powders. X-ray spectra from the resulting ingots show that they are mainly composed of $NdFe_2$ with a lattice parameter $a = 7.458$ Å (to be compared with Cannon *et al.* [1] : $a = 7.452$) together with a small amount of impurities which could not be identified : their spectral lines (at $d = 2.92$ Å, 2.73 Å, 2.53 Å, 1.79 Å) do not correspond to either Nd metal or Nd_2Fe_{17} or a hypothetical Nd_6Fe_{23}.

Recently Shimotomai *et al.* [8] have also succeeded in preparing $NdFe_2$ by applying 50 kbar pressure at 1 000 °C to a stoichiometric alloy of Nd and Fe; their product seems to be composed essentially of $NdFe_2$ but with a few percent of an impurity which may be Nd_6Fe_{23}.

3.1.2 *Curie temperature.* — ^{57}Fe Mössbauer spectroscopy shows that $NdFe_2$ in powder form rapidly decomposes upon heating. For this reason the measurements were performed on ingots which were contained in copper tubes sealed under vacuum at room temperature [12] which was sufficient to prevent any oxydation during the duration of the measurements (1-2 h). The temperature dependence of the magnetization in a field of 5 000 Oe is shown in figure 1. It gives,

$$T_c = 305 \pm 5\ ^{\circ}C \qquad (578 \pm 5\ K).$$

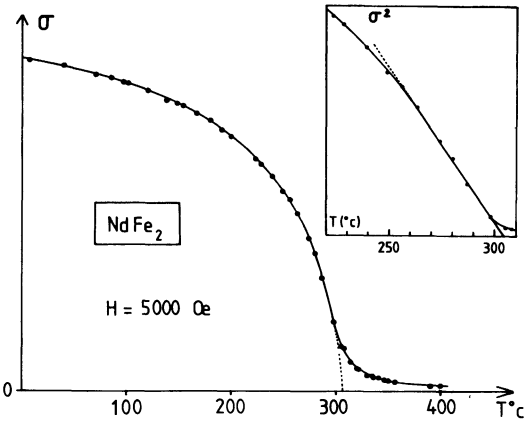

Fig. 1. — $NdFe_2$: determination of T_c.

3.1.3 *Magnetization measurements.* — As mentioned in the introduction, $NdFe_2$ is expected to be ferromagnetic ($\mu_{Nd} \parallel \mu_{Fe}$).

The electronic ground state of the Nd^{3+} ion is : $4f^3$, $^4I_{9/2}$, $S = 3/2$, $J = 9/2$, $g_J = 8/11$ [13] and its theoretical saturation moment is :

$$\mu_{sat} \equiv g_J \mu_B J = 3.27\ \mu_B .$$

It seems reasonable to assume that at helium temperature the Nd^{3+} moment is very nearly saturated (see the discussion in § 3.2 below) and that μ_{Fe} is $\sim 1.6\ \mu_B$ at helium temperature and $\sim 1.4\ \mu_B$ at room temperature as in the other RFe_2. Accordingly, for a ferromagnetic structure, the magnetic moment per formula unit should be about 6.5 μ_B at helium temperature and larger than 2.8 μ_B at room temperature. Obviously no compensation temperature is expected. On the other hand, if $NdFe_2$ were ferrimagnetic with the above values of the magnetic moments, there would exist a compensation point around helium temperature and upon raising the temperature, the magnetization would first increase.

According to experiment the temperature dependence of the remanent magnetization of our samples in a field of 1 000 Oe is small, except for a small decrease between 0 and 80 K, which might correspond to some unknown magnetic impurity. Magnetization isotherms in fields of up to 26 kG were also recorded. At 4.2 K and 50 K the samples are clearly far from saturation. At 300 K the extrapolated value of the magnetization is 57 ± 3 e.m.u./g. This result will be used for estimating the demagnetizing field $4\pi M$ in the high field experiments of § 3.5. For pure $NdFe_2$ such a magnetization would correspond to a moment of $\sim 2.6\ \mu_B$ per formula unit, although this value may be underestimated by a factor of about 1.5 since we started from an equiatomic mixture of Nd and Fe instead of the stoichiometric composition. These results suggest that $NdFe_2$ is indeed ferromagnetic at room temperature. Shimotomai *et al.* [8] report a magnetization of 4.6 μ_B per formula unit at 78 K in 15 kG which strongly suggests ferromagnetism at this temperature, although their sample is certainly not saturated by such a field (as shown by our own measurements and by the high field Mössbauer experiments of § 3.5 below).

3.2 NUCLEAR MAGNETIC RESONANCE EXPERIMENTS ON ^{143}Nd. — These experiments were made to determine the magnitude of the Nd^{3+} moment, which is of some interest in computing the theoretical dipolar parameter A_{dip}.

The N.M.R. signal in zero field (Bloch wall edges) at 1.4 K was readily obtained and is displayed in figure 2. For ^{143}Nd, $I = 7/2$. The hyperfine hamiltonian in an ordered magnetic state, referred to the magnetization direction OZ ($/\!/ \langle 110 \rangle$) has the following form

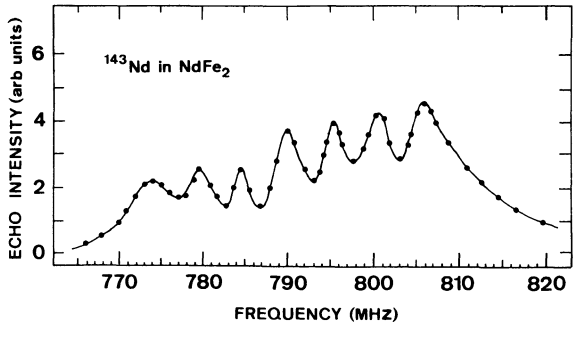

Fig. 2. — $NdFe_2$: N.M.R. spectrum of ^{143}Nd.

$$\mathcal{H}_{hf} = [A_J \langle J_Z \rangle - \hbar\gamma_n H_c] I_Z - \frac{e^2 Q(1 - R_Q) \langle J \| \alpha \| J \rangle \langle r^{-3} \rangle_{4f}}{4 I(2I - 1)} [\langle 3 J_Z^2 - J(J+1) \rangle (3 I_Z^2 - I(I+1)) + \langle 3 J_X^2 - J(J+1) \rangle (3 I_X^2 - I(I+1)) + \langle 3 J_Y^2 - J(J+1) \rangle (3 I_Y^2 - I(I+1))] \quad (5)$$

$$\mathcal{H}_{hf} \equiv - \hbar\gamma_n H_{eff} I_Z + P\left[3 I_Z^2 - I(I+1) + \frac{\eta}{2}(I_+^2 + I_-^2)\right] \quad (6)$$

in which :

$$H_{eff} = - A_J \langle J_Z \rangle \hbar\gamma_n + H_c . \quad (6')$$

In equation (6') the first term in $H_{eff}(- A_J \langle J_Z \rangle / \hbar\gamma_n)$ is associated with the 4f electrons and the second term (H_c) to the conduction electrons. There is no lattice contribution to the electric field gradient because the Nd^{3+} site has cubic symmetry. On the other hand because P is small compared with $\hbar\gamma_n H_{eff}$ (see below), the effect of the off diagonal terms in η is negligible.

From the N.M.R. spectrum one obtains :

$$\begin{cases} \nu_0 \equiv \left| \dfrac{g_n \mu_N H_{eff}}{h} \right| = (790 \pm 1)\ \text{MHz}, \\ \qquad\qquad \text{whence} \quad H_{eff} = 3\,390\ \text{kOe} \\ |P| = 2.3\ \text{MHz} . \end{cases}$$

These values are to be compared with the maximum contributions expected from the 4f shell in the fully polarized state $J_Z = J$:

$$\begin{cases} H_{max}^{4f} \equiv \left| \dfrac{A_J J}{\hbar\gamma_n} \right| = 4\,260 \pm 40\ \text{kOe} \\ P_{max} = - 5.3\ \text{MHz} . \end{cases}$$

Two possible explanations for the difference between H_{eff} and H_{max}^{4f} are :

1) the R.E. moment is reduced ($\langle J_Z \rangle < J$), which could arise if the crystalline field at the R.E. ion is not small compared with the Fe-R.E. exchange interaction ;

2) there are additional terms in H_{eff}. The correct explanation can be found considering the second half of the RFe_2 series :

— as concerns the magnitude of the R.E. moment, inelastic neutron scattering experiments on $ErFe_2$, $HoFe_2$, $TbFe_2$ [14], have been satisfactorily interpreted by assuming that the R.E. moment is saturated. A polarized neutron study of $HoFe_2$ [15] has led to a R.E. moment of 9.15 μ_B, close to the saturation value 10 μ_B. These results imply that the Fe-R.E. exchange interaction is much larger than crystal field effects. Since the Fe-R.E. exchange interaction is believed to be roughly constant throughout the series and since crystal field effects are not expected to be drastically bigger in the first half, it seems reasonable to conclude that the Nd moment is also saturated in $NdFe_2$, to within 5-10 % ;

— concerning the magnitude of the hyperfine field H_{eff}, as compared to the free ion value H_{max}^{4f}, table I shows that in the second half H_{eff} is always appreciably higher than H_{max}^{4f}. This has been interpreted by assuming [16] that H_{eff} has the form

$$H_{eff} = H_{max}^{4f} + H_{sp} + H_{tr}^{Fe} + H_{tr}^{R.E.}$$

in which the additional terms have the following interpretation :

— H_{sp} (self polarization field) represents the polarization of the conduction electrons by the R.E. itself. It consists of a contribution : $H_{sp}(\langle S^{R.E.} \rangle)$ proportional to $\langle S_Z^{R.E.} \rangle$, and possibly a second contribution : $H_{sp}(\langle L^{R.E.} \rangle)$ proportional to $\langle L_Z^{R.E.} \rangle$,

Table I. — *Comparison of the hyperfine fields at the Rare Earth nucleus in the free ion and in the* RFe_2 *compounds* : $\Delta H = H_{RFe_2} - H_{\text{Free ion}}$.

Rare Earth	Nd	Sm	Gd	Tb	Dy	Ho	Er	Tm	Yb
Free ion kOe [g]	4 253	3 409	− 323	3 148	5 715	7 291	7 705	6 647	4 173
RFe_2 kOe	3 390 [f]	3 042 [a]	+ 453 [c]	3 584 [b]	6 490 [b]	7 761 [d]	8 180 [b]	7 020 [b]	4 440 [e]
ΔH kOe	− 863	− 367	+ 776	+ 436	+ 775	+ 470	+ 475	+ 373	+ 267

([a]) VIJAYARAGHAVAN, R., SHIMIZU, K., ITOH, J., GROVER, A. K., GUPTA, L. C., *J. Phys. Soc. Japan* **43** (1977) 1854.

([b]) BERTHIER, Y., DEVINE, R. A. B., BUTERA, R., to be published in *Proc. of Symposium on Nuclear and Electron Resonance Spectroscopies Applied to Materials Science*, Boston, Nov. 1980.

([c]) GEGENWARTH, R. E., BUDNICK, J. I., SKALSKI, S., WERNICK, J. H., *Phys. Rev. Lett.* **18** (1967) 9.

([d]) MACKENZIE, I. S., MCCAUSLAND, M. A. H., WAGG, A. R., GUIMARAES, A. P., HOLDEN, E., BAILEY, S., *Proc. of 16th Ampere congress*, Bucharest 1970, p. 480.

([e]) MEYER, C., GROS, Y., HARTMANN-BOUTRON, F., CAPPONI, J. J., *J. Physique* **40** (1979) 403.

([f]) This paper.

([g]) BLEANEY, B., in *Magnetic Properties of Rare Earth*, ed. by R. J. Elliott (Plenum) 1972, chap. 8 : Hyperfine Interactions.

— H_{tr}^{Fe} is a transferred hyperfine field due to the iron which is responsible, for example, for the hyperfine field of ~ 220 kG observed at the ^{89}Y nucleus in YFe_2 [10],

— $H_{tr}^{R.E.}$ is a transferred field from the R.E. which is small (~ 20 kG).

The positive discrepancy between H_{eff} and H_{max}^{4f} in the second half of the series is probably mainly due to $H_{sp}(\langle S^{R.E.} \rangle)$ and to H_{tr}^{Fe}. In the first half of the series the relative orientations of $\langle S^{R.E.} \rangle$ with respect to $\langle J \rangle$ and of μ_{Fe} with respect to $\mu_{R.E.}$ are opposite those in the second half; the signs of $H_{sp}(\langle S^{R.E.} \rangle)$ and H_{tr}^{Fe} should therefore be changed relative to H_{max}^{4f} and the difference $\Delta H = H_{eff} - H_{max}^{4f}$ should become negative : the signs and magnitudes of ΔH for $NdFe_2$ and $SmFe_2$ in table I seem to corroborate this interpretation.

The quadrupole coupling P is also appreciably smaller than P_{max}, but this may not be significant, because even slight lattice strains could create contributions of the order of a few MHz, which will modify the apparent P.

These considerations indicate that the Nd moment in $NdFe_2$ is probably very nearly saturated : this will be of importance in computing the theoretical dipolar parameter A_{dip} and the demagnetizing fields.

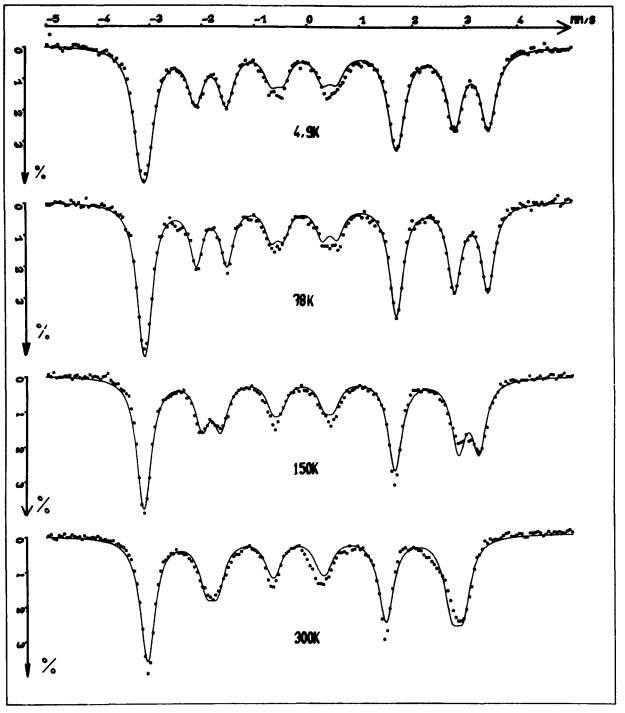

Fig. 3. — $NdFe_2$: ^{57}Fe Mössbauer spectra. The full curves are theoretical fits.

3.3 ^{57}Fe MÖSSBAUER SPECTRA IN ZERO FIELD. — Figure 3 shows some ^{57}Fe spectra of enriched $NdFe_2$. At low temperatures they exhibit a decomposition into 2 : 2 subspectra which is characteristic of a magnetization lying along [110]. This decomposition disappears rather abruptly around 150 K, leaving only three broadened lines. We tentatively interpret this change in the spectra as resulting from a rotation of the magnetization from [110] towards [100] (similar conclusions have been arrived at by Shimotomai *et al.* [8]). Computer fits were performed at all temperatures. Since A/H_n is large it is necessary to use the exact formulas ([7], p. 145) instead of the approximate first order expressions of reference [2]. The complete results of the fits are displayed in table II in which H_I and H_{III} denote the magnitudes of the total hyperfine fields ($\mathbf{H}_n + \mathbf{H}_d$) at the two types of inequivalent sites ; θ'_I and θ'_{III} are the angles these fields make with the corresponding $\langle 111 \rangle$ directions and φ is the angle of the magnetization with [100] in the xOy plane. In particular :

— at 4.2 K :

$\varphi = 45°$, $e^2 qQ/2 = -0.64 \pm 0.02$ mm/s,

$H_n = 189 \pm 1$ kOe, $A = 14 \pm 1$ kOe,

— at 300 K :

$\varphi = 11 \pm 3°$, $e^2 qQ/2 = -0.65 \pm 0.05$ mm/s,

$H_n = 174 \pm 1$ kOe, $A = 11 \pm 3$ kOe.

Table II. — *Results of the computer fits of the* ^{57}Fe *Mössbauer spectra in* $NdFe_2$.

T (K)	δ mm/s	$\frac{\Gamma}{2}$ mm/s	$\frac{e^2 qQ}{2}$ mm/s	H_{III} kOe	H_I kOe	θ'_I	θ'_{III}	H_n kOe	A_d kOe	φ
4.9	− 0.037	0.17	− 0.64	203.1	176.4	42°	90°	189	14	45°
40	− 0.037	0.145	− 0.64	202.7	176.5	42°	90°	189	13.6	45°
78	− 0.044	0.145	− 0.65	202.2	176.8	42°	90°	189	13	45°
115	− 0.056	0.14	− 0.63	201.5	177	41°	90°	189	12.7	45°
131	− 0.068	0.151	− 0.63	200.5	177.2	41°	90°	188.5	12	45°
150	− 0.083	0.162	− 0.6	196	181	46°	77°	188	11	22°
160	− 0.086	0.165	− 0.65	194	182	49°	72°	187	10	19°
225	− 0.12	0.163	− 0.66	189	180	52°	69°	184	10	13°
298	− 0.166	0.173	− 0.65	182	174	53°	67°	177	11	11°

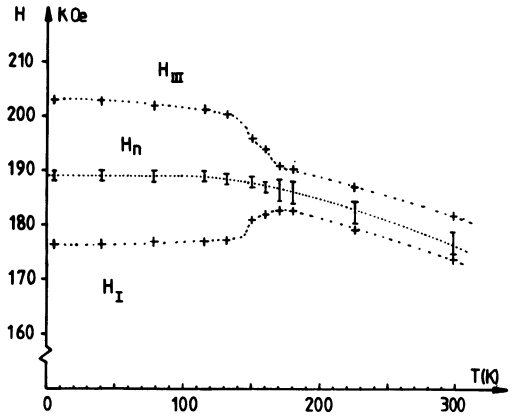

Fig. 4. — $NdFe_2$: temperature dependences of the hyperfine fields H_I, H_{II} and H_n at the ^{57}Fe nucleus.

The temperature dependences of H_I, H_{III} and H_n are shown in figure 4. As expected, the isotropic field H_n does not exhibit any discontinuity at the reorientation temperature.

Let us now compare A and A_{dip}. At 4.2 K, using $\mu_{Nd} = 3.27\ \mu_B$ and $\mu_{Fe} = 1.6\ \mu_B$, one predicts that the computed dipolar parameter, $A_{dip} = 0.05$ kG for the expected ferromagnetic structure and $A_{dip} = 4.1$ kG for an hypothetical ferrimagnetic one. At room temperature, if one assumes that Nd^{3+} sees only an exchange coupling (Eq. (1)) :

$$\mathcal{H}_{ex} \equiv -2(g_J - 1)\,\mathcal{J}_{ex}\,\mathbf{S}.\mathbf{J} \equiv -2(g_J - 1)\,\mu_B\,\mathbf{H}_{ex}.\mathbf{J} \tag{7}$$

with $100\ K \lesssim \mu_B H_{ex}/k_B \lesssim 200$ K, and that $\mu_{Fe} \simeq 1.4\ \mu_B$, one predicts that $A_{dip} \lesssim 1.3$ kG in the ferromagnetic case and $A_{dip} \lesssim 3$ kG in the ferrimagnetic case. These values are to be compared with the experimental results : $A \simeq 14$ kG at 4.2 K and $A \simeq 11$ kG at 300 K.

Two possible explanations for these discrepancies are :

1) the magnetic structure is anomalous, and is neither ferromagnetic, nor ferrimagnetic. This can be checked by neutron diffraction experiments, as discussed in the following section,

2) there exists an intrinsic anisotropy of the hyperfine structure in addition to the dipolar contribution, as suggested in [3] (Appendix II) and [6], and as discussed in § 6.3.2 below.

The following section, concerned with neutron diffraction experiments, will show that the first explanation is not possible because the magnetic structure can only be ferro or ferrimagnetic. The ferromagnetic character is then confirmed by high field Mössbauer experiments which also provide additional and independent determinations of A and $e^2\,qQ/2$.

3.4 NEUTRON DIFFRACTION EXPERIMENTS. — It is possible to show that an antiferromagnetic arrangement of the R.E. moments of the type shown in figure 5, with the R.E. moments parallel to [110], will create a dipolar field of the order, 20 kG, at half the iron sites and of the order zero at the other half, as compared with the iron contribution (± 2 kG). However such an arrangement seems unlikely because it is inconsistent with all current theories and also because it would raise difficult problems concerning the molecular field description in terms of Fe-R.E. and R.E.-R.E. exchange. Indeed, for such a structure to exist, the R.E.-R.E. exchange would probably have to be larger than the R.E.-Fe exchange; this is quite unlikely in the RFe_2 series. In addition, as pointed out by Dr. E. F. Bertaut, in the presence of the large Fe-Fe exchange a realistic structure would probably consist of ferromagnetic iron moments at right angles to the, slightly canted, antiferromagnetic Rare Earth moments. The total magnetic moment of such a structure would not be zero and it could be rotated by an applied field.

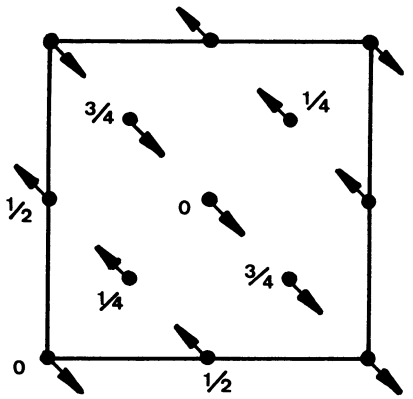

Fig. 5. — $NdFe_2$: antiferromagnetic arrangement of the Nd moments which gives rise to a large dipolar field at the iron.

Neutron diffraction experiments were performed at the high flux reactor at the I.L.L. because of the small amount of product available : 1 g. The experiments were upset by various experimental failures of the D2 cryostat, which are described in detail in [7] (p. 65 and 129) and which are responsible for the poor quality of the results. For this reason we only show in figure 6 the spectrum of $NdFe_2$ at 4.2 K in zero field and the difference between this spectrum and the spectrum in 40 kG. The difference spectrum does not exhibit any of the magnetic neodymium superstructure lines (such as 001, 110, 201, 003, 221, 203, 312, etc...) expected for the unconventional structure described above, and is only compatible with a ferro or a ferrimagnetic structure. The results are not good enough to distinguish between these two possibilities (see reference [7] for more details).

Other techniques can distinguish between ferro and ferrimagnetic structures. The magnetization measurements by Shimotomai *et al.* [8], and the high field Mössbauer experiments to be described below, both show that $NdFe_2$ is indeed ferromagnetic.

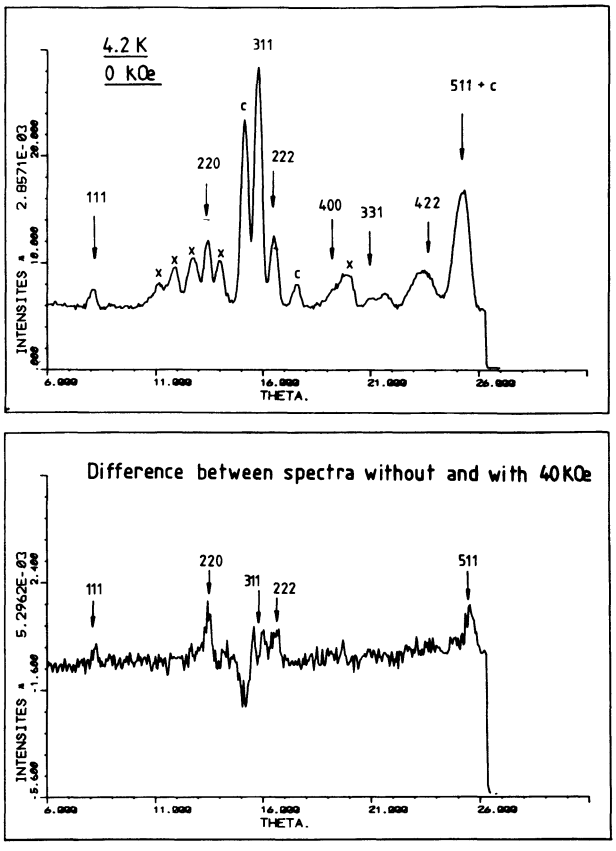

Fig. 6. — $NdFe_2$: neutron diffraction spectra. Top : spectrum at 4.2 K in zero field ; bottom : difference between spectra without and with a 40 kG field. The lines marked with a X are impurity lines as previously seen in the X-ray spectra. Cryostat line (Al) are indicated (c).

3.5 HIGH FIELD ^{57}Fe MÖSSBAUER EXPERIMENTS (PERFORMED AT S.N.C.I. AND C.E.N.G. IN COLLABORATION WITH O. MASSENET AND J. CHAPPERT [6]). — These experiments were made on pellets of rigidly supported powders in fields of 45-60 kG ([1]). Most of their results have been reported briefly in reference [6].

— At room temperature, where the anisotropy is small, the magnetization of all the grains is aligned along the external field $\mathbf{H}_0$ (parallel to the γ ray). The two intermediate Mössbauer lines disappear and the remainder exhibit an inhomogeneous broadening, from which $e^2\,qQ/2$ and A can be extracted by computer fitting.

— At 4.2 K the anisotropy is so large that the field can only remove the Bloch walls and align the magnetization in each grain along the closest easy axis : the intermediate lines diminish, but they do not vanish. The fits were made with this assumption.

According to the M.E. spectra the applied field $\mathbf{H}_0$ opposes the hyperfine field, which means that μ_{Fe} is parallel to $\mathbf{H}_0$, as expected if $NdFe_2$ is ferromagnetic, or ferrimagnetic with $|\mu_{Nd}| < 2\,|\mu_{Fe}|$. The total field seen by the ^{57}Fe nucleus is (see Appendix) then given by,

$$H = H_n - H_0 + 4\pi M$$

where $4\pi M$ is the demagnetizing field of the pellet.

At room temperature the fits give [6] :

$$A \sim 14 \pm 2\,\text{kOe}, \quad e^2\,qQ/2 \sim -0.4 \pm 0.1\,\text{mm/s}$$

in fair agreement with the values obtained in zero field :

$$A = 11 \pm 3\,\text{kOe}, \; e^2\,qQ/2 = -0.65 \pm 0.05\,\text{mm/s}\,.$$

The demagnetizing field is found to be equal to 12 ± 4 kOe instead of 6 kOe computed with the measured magnetization 57 e.m.u./g (note however that the determinations are not very precise and the samples were not the same).

At helium temperature one finds that

$$A = 14\,\text{kOe}, \qquad e^2\,qQ/2 = -0.6\,\text{mm/s}$$

which is also in good agreement with the zero field results. The demagnetizing field in this case is given by

$$4\pi M \overline{\cos\beta}$$

where β is the angle between the field and the closest easy axis in each grain. Using the computed value $\overline{\cos\beta} = 0.913$, one obtains a corrected demagnetizing field

$$4\pi M = 9.6\,\text{kOe}$$

whereas the computed $4\pi M$ for pure $NdFe_2$ (with $\mu_{Nd} \simeq 3.2\,\mu_B$, $\mu_{Fe} = 1.6\,\mu_B$) is as follows,

$$4\pi M = 14.5\,\text{kG if ferromagnetic}$$
$$4\pi M \simeq 0\;\text{kG if ferrimagnetic}\,.$$

Even if one allows for impurity effects, the above value of $4\pi M$, together with the magnetization results, clearly prove that $NdFe_2$ is ferromagnetic.

It follows that the discrepancy between the theoretical value A_{dip} and the experimental value A of the hyperfine anisotropy parameter A_d in $NdFe_2$ is a real one. We will discuss this problem in § 6.3.2.

4. **Additional results for $PrFe_2$.** — Preliminary results concerning the preparation and ^{57}Fe Mössbauer spectra of $PrFe_2$ were reported in reference [4]. The properties of $PrFe_2$ have been studied more recently by Shimotomai *et al.* [9]. Note that the lowest electronic state of the Pr^{3+} ion is [13] :

$$Pr^{3+} : 4f^2\,, \quad {}^3H_4\,, \quad S = 1\,, \quad J = 4\,,$$
$$g_J = 4/5\,, \quad \mu_{sat} = 3.2\,\mu_B\,.$$

([1]) High field spectra on RFe_2 compounds were first taken by Wertheim [17] and Guimaraes [18], but without quantitative interpretation.

4.1 PREPARATION, CURIE TEMPERATURE, MAGNETIZATION MEASUREMENTS. — 4.1.1 *Preparation.* — In the same way as for $NdFe_2$ the preparation was made from an equiatomic mixture. The resulting product is not very pure, as is shown by figure 7 where the iron metal lines can be seen in addition to those of $PrFe_2$. The lattice parameter of our samples is in agreement with that of Cannon *et al.* [1].

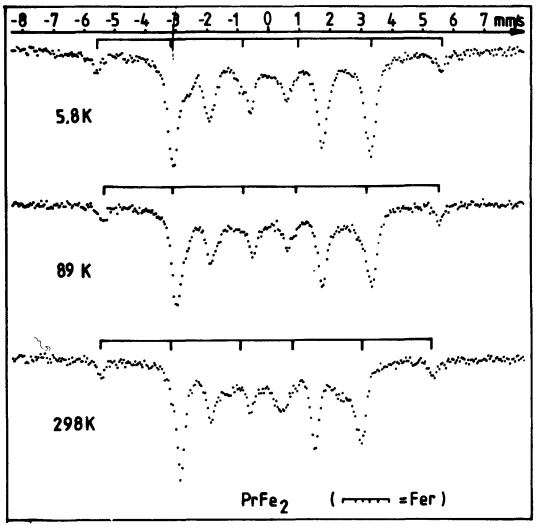

Fig. 7. — $PrFe_2$: ^{57}Fe Mössbauer spectrum in zero field.

4.1.2 *Curie temperature.* — Just as $NdFe_2$ decomposes rapidly upon heating so does $PrFe_2$. The Curie temperature, measured with the same method as for $NdFe_2$ is (see Fig. 8), as follows :

$$T_c = 270 \pm 10\ ^{\circ}C \qquad (543 \pm 10\ K).$$

4.1.3 *Magnetization measurements.* — We did not perform magnetization experiments on our own samples because of the iron impurities. The samples of Shimotomai *et al.* [9] apparently do not contain iron and Shimotomai *et al.* find a magnetization of 4.7 μ_B per formula unit at 78 K in 15 kG, as compared with the theoretical value of 6.4 μ_B (computed with $\mu_{Pr^{3+}} = 3.2\ \mu_B$, $\mu_{Fe} = 1.6\ \mu_B$) : this indicates ferromagnetism.

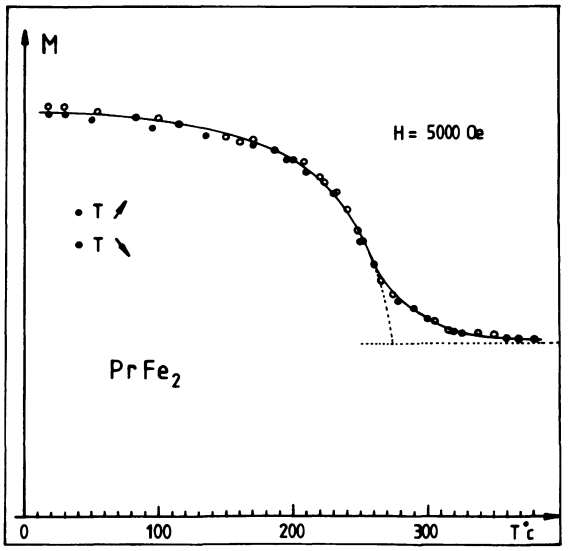

Fig. 8. — $PrFe_2$: determination of T_c.

4.2 ^{57}Fe MÖSSBAUER STUDY. — The ^{57}Fe Mössbauer spectra of $PrFe_2$ are shown in figure 7. Their aspect is the same as in figure 1 of [9] and suggests the presence of some unknown impurities in addition to the iron. At 4.2 K the widths of homologous lines are comparable, which would indicate a [100] magnetization direction. Along this direction, however, the spectrum is expected to be nearly pure Zeeman while the experimental spectrum exhibits an important apparent positive quadrupole effect :

$$\varepsilon = \frac{e^2 qQ}{4}(3\cos^2\theta' - 1) = +\ 0.4\ \text{mm/s}\,.$$

There are three possible explanations :

a) The apparent quadrupole effect could be due to « tipping effects » associated with a huge h.f.s. anisotropy $A \sim 35$ kOe [4]. This possibility is not consistent with the high field experiments to be described below.

b) The trigonal E.F.G. is enhanced with respect to the other RFe_2 : $e^2 qQ/2 = -\ 1.5$ mm/s instead of $-\ 0.5$ mm/s.

c) There is an induced E.F.G. collinear to the magnetization. Such a gradient was invoked in the interpretation of the spectra of ^{57}Fe impurities in $NdCo_2$, $HoCo_2$ and $GdCo_2$ [19, 20] and also in reference [9] relative to $PrFe_2$.

The hyperfine field derived by fitting the spectra at 4.2 K using assumption *b*) is $H_n = 190$ kG, in good agreement with the value $H_n = 192.4 \pm 1$ kG obtained by Shimotomai *et al.* using assumption *c*).

At room temperature the spectra possibly indicate a [111] magnetization direction, but we did not succeed in obtaining good fits because of the unknown spectrum due to impurities other than the iron impurities.

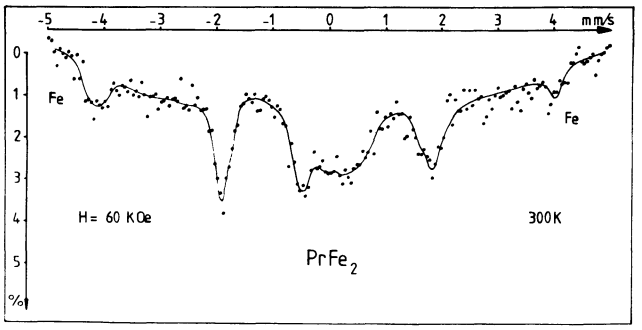

Fig. 9. — $PrFe_2$: ^{57}Fe Mössbauer spectrum in 60 kOe at room temperature. The full line is only a guide to the eye.

Note that the fits of reference [9] were made by adding to the computed $PrFe_2$ spectrum, absorption peaks of independent intensity, position, and width, which are intended to mimic an impurity phase. However at 4.2 K and 78 K this extra spectrum (dotted curves in figure 1 of [9]) does not really look like a Zeeman spectrum (there is a line « missing » on the right). In addition, if the impurities were Pr_2Fe_{17} or an hypothetical Pr_6Fe_{23}, the hyperfine field would probably be of the order 300 kG and not 200 kG (see tables A.2*c* and A.2*d* of Buschow's review paper [21*e*] p. 1246-1247).

Finally the average hyperfine field in figure 2 of [9] exhibits a discontinuity at the reorientation temperature which is surprizing because, as can be shown from equations (B.4) of Appendix II of [3], this average field is equal to the isotropic field H_n to within terms of the order $A^2/H_n \lesssim 1$ kOe.

The high field ^{57}Fe Mössbauer spectrum at room temperature (S.N.C.I.) is shown in figure 9. Because of its poor quality, only very rough adjustments could be made, leading to $A \sim 6$ kOe and

$$e^2 qQ/2 \sim -0.2 \text{ mm/s [6]}.$$

The main conclusion is that A is small, although larger than $A_{dip} \lesssim 2$ kOe.

5. **Additional results for $YbFe_2$.** — 5.1 PREVIOUS RESULTS. — The preparation, magnetization curves and ^{57}Fe Mössbauer study of $YbFe_2$ are described in detail in reference [2], the ^{170}Yb Mössbauer study in reference [3] and a brief report on the high field ^{57}Fe Mössbauer spectra is given in reference [6].

The most important results obtained prior to this study are the following :

— Yb is trivalent in $YbFe_2$. Note that Yb^{3+} has an electronic ground state : $4f^{13}$, $^2F_{7/2}$, $S = 1/2$, $J = 7/2$, $g_J = 8/7$, $\mu_{sat} = 4\,\mu_B$.

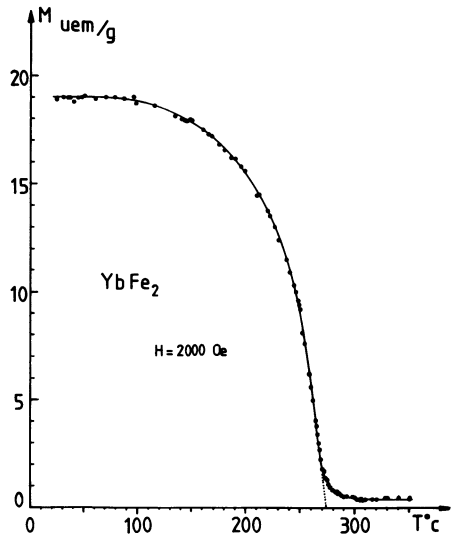

Fig. 10. — $YbFe_2$: determination of T_c.

— $YbFe_2$ is ferrimagnetic with a compensation temperature $T_{comp} \sim 31$ K [2].

— According to the zero field ^{57}Fe Mössbauer spectra the iron magnetization direction lies along [100] at 4.2 K. Above 50 K the magnetization deviates slightly from this direction within the (001) plane ($\varphi \sim 10°$ at 300 K [2, 7]).

— According to the temperature dependences of $\langle J_Z \rangle$ and $\langle 3J_Z^2 - J(J+1) \rangle$ ([2]), derived from ^{170}Yb Mössbauer spectra between 0 and 60 K, the crystalline field effects at the Yb^{3+} ion are negligible compared with the Fe-Yb exchange coupling ($|A_4\langle r^4 \rangle|, |A_6\langle r^6 \rangle| < 4$ K, $\mu_B H_{ex} = 111 \pm 4$ K) [3].

From the known variation of $\langle J_Z \rangle$, it is possible to obtain the iron moment at the compensation temperature $|\mu_{Fe}| = (1/2)|\mu_{Yb}| = 1.64 \pm 0.04\,\mu_B$ at 31 K [3].

5.2 EXPERIMENTS AROUND THE CURIE TEMPERATURE. — The Curie temperature was derived from the magnetization curves, in the same way as for $NdFe_2$ and $PrFe_2$. According to figure 10 :

$$T_c = 270 \pm 5\ °C \qquad (543 \pm 5\ K).$$

The Curie temperature could also be determined from ^{57}Fe Mössbauer experiments, in spite of the slow decomposition of $YbFe_2$ into iron metal upon heating. The spectrum at 290 °C is displayed in figure 11. It only exhibits a quadrupole doublet with

$$|e^2 qQ/2| = 0.45 \pm 0.05 \text{ mm/s}$$

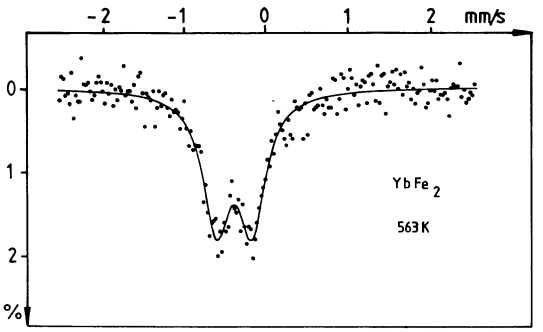

Fig. 11. — $YbFe_2$: ^{57}Fe Mössbauer spectrum at 290 °C (above T_c).

as compared with $e^2 qQ/2 = -0.5$ mm/s at room temperature (obtained by computer fitting of the magnetic spectra). By contrast a magnetic hyperfine structure can be seen in the spectra taken at 250 °C and 200 °C. The temperature dependence of the hyperfine field is shown in figure 12. It gives a Curie point of ~ 530 K (257 °C) in good agreement with the preceding determination.

5.3 HIGH FIELD ^{57}Fe MÖSSBAUER EXPERIMENTS. — From the high field spectrum at room temperature,

([2]) OZ is an axis parallel to $\langle J \rangle$, which is parallel to [100].

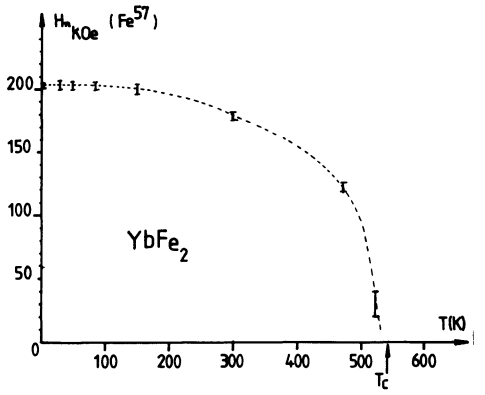

Fig. 12. — $YbFe_2$: temperature dependence of the ^{57}Fe hyperfine field.

given in reference [6], one obtains : $9 < A < 14$ kOe, $e^2\,qQ/2 \sim -0.3 \pm 0.1$ mm/s, as compared with the values obtained in zero field : $A = 12 \pm 5$ kOe, $e^2\,qQ/2 = -0.5 \pm 0.1$ mm/s, and a demagnetizing field $4\,\pi M = 11 \pm 5$ kOe, as against 6 kOe calculated from the magnetic moment of $(2 \pm 0.25)\ \mu_B$ per formula unit [2].

The spectrum at 4.2 K (Fig. 13), shows that, in contrast with the room temperature behaviour [6], the applied field adds to the hyperfine field, as follows :

$$H = H_n + H_0 - 4\,\pi M\,.$$

This means that $\mu_{Yb} > 2\,\mu_{Fe}$, in agreement with the existence of a compensation point at 31 K. The theoretical fit, figure 13, was made in the same way as for $NdFe_2$ and gives $A \sim 7$ kOe and $e^2\,qQ/2 \sim -0.5$ mm/s in agreement with the zero field values $A = 7 \pm 2.5$ kOe and $e^2\,qQ/2 = -0.5 \pm 0.1$ mm/s. The demagnetizing field, both theoretically and experimentally is very small : $4\,\pi M \sim 2$ kOe. While the calculated line positions are in good agreement with experiment,

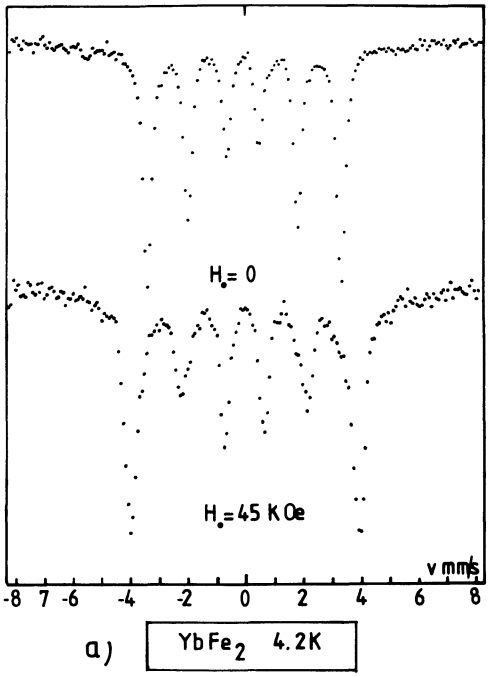

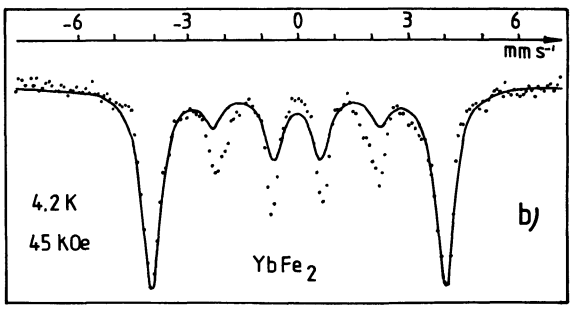

Fig. 13. — *a*) Comparison of the Mössbauer spectra at 4.2 K without and with a 45 kOe field ; *b*) Theoretical fit of the spectrum at 45 kG.

Table III. — *Curie temperatures across the* RFe_2 *series.*

			T_c (K) in the RFe_2 series					
R^{3+}	$4f^n$	$(g_J-1)^2\,J(J+1)$	Ref. [21*a*]	Ref. [21*b*]	Ref. [21*c*]	Ref. [21*d*]	Ref. [21*e*]	This work
Pr	2	0.8						543
Nd	3	1.84						578
Sm	5	4.46	688	676		674	688	
Gd	7	15.75	782	785	798		796	
Tb	8	10.5	705	711		694	704	
Dy	9	7.08	638	635		630	635	
Ho	10	4.5	614	612		594	608	
Er	11	2.55	596	590		571	587	
Tm	12	1.17	610			555	599	
Yb	13	0.32						543
Lu	14	0	610		583	562	596	
Y			542	543	537	528	542	

the theoretical intensities of the inner lines are too small which may be due to the numerical approximations made in the calculation, which are discussed in reference [7], p. 155-159.

We have found that the h.f.s. anisotropy parameter is approximately, $A = 7.5 \pm 2.5$ kOe at 4.2 K and $A \sim 12 \pm 2.5$ kOe at 295 K. These experimental values are to be compared with the theoretical dipolar values A_{dip} which can be computed with the known magnetic moments. At 4.2 K, $\langle J \rangle = J$ which means that $\mu_{Yb} = 4\,\mu_B$, and $\mu_{Fe} = 1.64 \pm 0.04\,\mu_B$ (see § 5.1), whence $A_{dip} = 5 \pm 0.06$ kOe. At 295 K, $\mu_{Yb} = 0.6\,\mu_B$ (computed with the Fe-Yb exchange field determined at low temperature) and $\mu_{Fe} = 1.44 \pm 0.06\,\mu_B$ (deduced from the value at helium temperature by assuming that $\mu_{Fe} \propto H_n$), whence $A_{dip} = 2.4 \pm 0.1$ kOe. While at 4.2 K, $A \sim A_{dip}$ within the experimental error, in contrast at ^{295}K, $A \gg A_{dip}$. As in $NdFe_2$ there is a discrepancy between A and A_{dip}. We will return to this point in § 6.3.2.

6. **General survey and discussion.** — In this section we review the results obtained on $YbFe_2$, $NdFe_2$, $PrFe_2$, in the light of the properties already known about RFe_2.

6.1 MAGNETIC STRUCTURE AND CURIE TEMPERATURES. — While the second half of the RFe_2 series is ferrimagnetic, the magnetization measurements by Shimotomai *et al.* [8, 9], and our own work, both show that $PrFe_2$ and $NdFe_2$ are ferromagnetic, as expected for the first half RFe_2.

In table III are collected Curie temperatures of the whole series, as measured by various authors [21]. These are plotted in figure 14*a* as a function of the number of 4f electrons. According to a naive model based on equation (1), T_c is expected to vary linearly as $(g_J - 1)^2\, J(J+1)$ [21 *bis*]. This is shown in figure 14*b*. $SmFe_2$ deviates from this law, probably because of *J-J* mixing in the Sm^{3+} ion. The measured values for $TmFe_2$ and $LuFe_2$ seem a little high, with the exception of reference [21*d*].

6.2 CRYSTALLINE FIELD EFFECTS. — With the exception of YFe_2, $GdFe_2$ and $LuFe_2$ the magnetocrystalline anisotropy of the RFe_2 is mainly due to the cubic crystalline field acting on the R.E. ion, whose hamiltonian has the following form,

$$\mathcal{H}_c = A_4 \langle r^4 \rangle \langle J \| \beta \| J \rangle (O_4^0 + 5\,O_4^4) + \\ + A_6 \langle r^6 \rangle \langle J \| \gamma \| J \rangle (O_6^0 - 21\,O_6^4)\,. \quad (8)$$

Previous anisotropy measurements on single crystals of $TmFe_2$ and $TbFe_2$, and studies of ternary phase diagrams in the second half of the series seemed to suggest that A_4 and A_6 were constant throughout the series, with [3] :

$$\frac{A_4\, a_0^4}{k_B} \sim +\,40\ \text{K}\,, \qquad \frac{A_6\, a_0^6}{k_B} \sim -\ \text{a few K}\,.$$

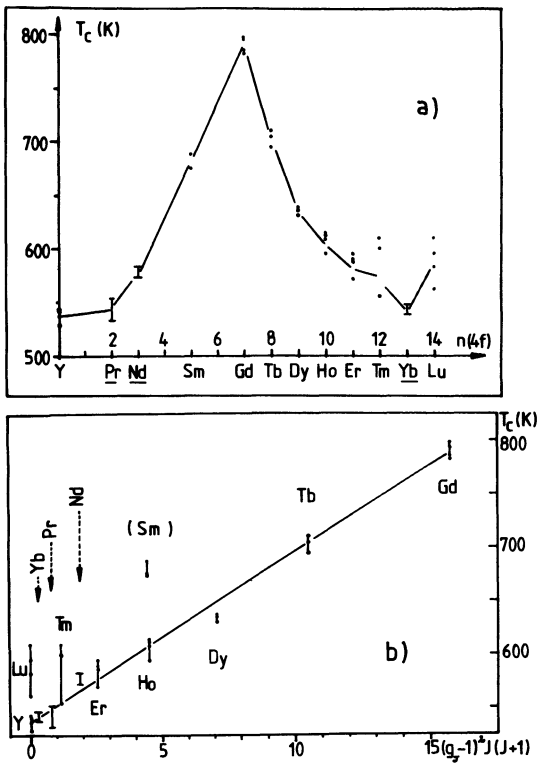

Fig. 14. — *a*) Plot of the Curie temperature T_c across the RFe_2 series ; *b*) Plot of T_c *versus* $(g_J - 1)^2\, J(J+1)$.

However, in contradiction with this result a Mössbauer study of ^{170}Yb in $YbFe_2$ shows that in this compound both $|A_4 \langle r^4 \rangle|$, and $|A_6 \langle r^6 \rangle|$ are very small (< 4 K) [3].

Moreover it can be shown that the $\langle 110 \rangle$ magnetization direction observed in $NdFe_2$ [5] and $SmFe_2$ [22] means that $|A_6 \langle r^6 \rangle| \sim A_4 \langle r^4 \rangle$. In addition Shimotomai *et al.* find that the magnetization directions in $PrFe_2$ can only be accounted for if A_4 and A_6 are both negative [9].

Thus it follows that A_4 and A_6 are not constant throughout the series. For a more detailed discussion, including the possible roles of magnetostriction and anisotropic exchange, see references [3, 5].

6.3 MAGNETIC HYPERFINE STRUCTURE AT THE IRON NUCLEUS. — 6.3.1 *Isotropic field.* — As discussed in detail in the Appendix, the apparent isotropic hyperfine field H_n introduced in § 2.3 is expected to have the form,

$$H_n = H_{iso} \mp \frac{4\pi}{3v}\,\mu_B\, g_J \langle J_{R.E.} \rangle \quad (9)$$

$$H_{iso} = A' \langle S_{Fe} \rangle + B\,|(g_J - 1) \langle J_{R.E.} \rangle| \quad (10)$$

in which $\mp\, 4\pi\mu_B\, g_J \langle J_{R.E.} \rangle / 3v$ is a Lorentz correction not previously considered and H_{iso} is the « true » isotropic hyperfine field, which is the sum of an intrinsic term, $A' \langle S_{Fe} \rangle$, and of a transferred contribution from the R.E., proportional to the R.E. spin, $B\,|(g_J - 1) \langle J_{R.E.} \rangle|$.

At 0 K, $\langle J_{R.E.} \rangle \simeq J$ and, assuming $A' \langle S_{Fe} \rangle$ to be constant throughout the series, $(H_{iso})_{0K}$ should be a linear function of $|(g_J - 1)J|$. We obtained $(H_{iso})_{0K}$ by subtracting the computed value of the Lorentz contribution from the experimental value of $(H_n)_{0K}$ (Table IV). As is shown in figure 15*a*, a linear law is approximately obeyed in the second half of the series (with $A' \langle S_{Fe} \rangle = 202.7$ kG and $B = 6.2$ kG), but the data points relating to the first half of the series strongly deviate from such a law.

For this reason we introduced a transferred contribution proportional to the orbital moment of the Rare Earths : $\langle \mathbf{L}_{R.E.} \rangle = (2 - g_J) \langle \mathbf{J}_{R.E.} \rangle$ ([3]). It then follows that,

$$H_{iso} = A' \langle S_{Fe} \rangle + B |(g_J - 1) \langle J_{R.E.} \rangle| \mp \mp C |(2 - g_J) \langle J_{R.E.} \rangle| \quad (11)$$

(− in the first half, + in the second half).

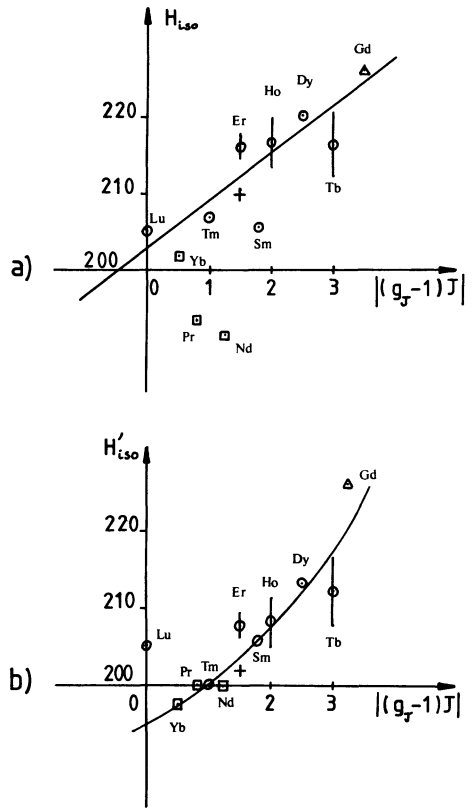

Fig. 15. — *a*) Plot of $(H_{iso})_{0K}$, kG, (Eqs. (9, 10) and Table IV) *versus* $|(g_J - 1)J|$. *b*) Plot of $(H'_{iso})_{0K}$, kG, (Eq. (12)) *versus* $|(g_J - 1)J|$. The data points are derived from the experimental values of H_n (0 K) as described in the text. The data points marked with □, ○, △ and + are respectively derived from H_n (0 K) of References *a*, *b*, *c*, *d* in table IV. The straight line in figure 15*a* is a least squares fit not including Gubbens' data point + (which was added later).

([3]) A polarization of the conduction band by the orbital moment of the R.E. has been invoked to explain the hyperfine field at the R.E. nucleus [23*a*] and an anisotropic orbital polarization has now been included in such a theory [23*b*].

Table IV.

	H_n (0 K)		H_{iso} (0 K)
$PrFe_2$	191 ± 1	([a])	193.4 ± 1
$NdFe_2$	189 ± 1	([a])	191.5 ± 1
$SmFe_2$	205 ± 2	([b])	205.5 ± 2
$GdFe_2$	231	([c])	226
$TbFe_2$	223.2 ± 4.5	([b])	216.2 ± 4.5
$DyFe_2$	228	([b])	220.1
$HoFe_2$	224.5 ± 3.5	([b])	216.5 ± 3.5
$ErFe_2$	223.1 ± 1.5	([b])	215.9 ± 1.5
	217	([d])	209.8
$TmFe_2$	212.5	([b])	206.8
$YbFe_2$	205 ± 1	([a])	201.7 ± 1
$LuFe_2$	205	([b])	205

Values of H_n (0 K) and H_{iso} (0 K) used in figure 15. H_{iso} (0 K) is deduced from H_n (0 K) as described in the text.

([a]) Present work.

([b]) Average of the values at 4.2 and 80 K in Buschow's review paper (Ref. [21*e*] p. 1245) ; the error bar corresponds to the dispersion around this average.

([c]) Measured on figure 1*c* of Mizoguchi *et al.* [35].

([d]) Gubbens (private communication).

In figure 15*b* we plot the following

$$(H'_{iso})_{0K} \equiv (H_{iso})_{0K} \pm C |(2 - g_J) \langle J_{R.E.} \rangle| \quad (12)$$

(with $C = 1.39$ kG) *versus* $|(g_J - 1)J|$. With the exception of $LuFe_2$ the data points for the whole series lie close to an almost linear curve (Fig. 15*b*). This tentatively suggests the existence of both spin and orbital transferred contributions to H_n : indeed the constant C was determined using the H_{iso} of Nd, Pr and Tm which have approximately the same $|(g_J - 1)J|$. Thus the only check in the first half of the series is provided by the Sm data point, which may be unrepresentative because of *J-J* mixing. The deviation of the $LuFe_2$ data point from the curve may be correlated with the high T_c of $LuFe_2$ compared with that of $YbFe_2$.

6.3.2 *Anisotropic contribution.* — We have seen that in $NdFe_2$ at any temperature the theoretical dipolar constant A_{dip} is much smaller that the experimental value A. A similar important discrepancy between A and A_{dip} seems also to exist in $YbFe_2$ at room temperature. More generally, as shown by table V, A_{dip} seems to be smaller than A throughout the whole series, the effect being largest for $NdFe_2$ and $SmFe_2$.

As suggested in reference [3], Appendix II, a possible explanation for this phenomenon could be the existence of an intrinsic anisotropy of the hyperfine structure of the iron, which could be written, with respect to the local trigonal axis OZ, in the following way,

$$\mathcal{H}^{hf}_{an} = -\hbar\gamma_n \left[\mathcal{A}^{hf}_{\parallel} \frac{\boldsymbol{\mu}^{\parallel}_{Fe}}{\mu_B} \cdot \mathbf{I}^{\parallel} + \mathcal{A}^{hf}_{\perp} \frac{\boldsymbol{\mu}^{\perp}_{Fe}}{\mu_B} \cdot \mathbf{I}^{\perp} \right]. \quad (13)$$

Table V. — (*Reproduced from reference* [6]). *Computed value* A_{dip} *and experimental value A of the* ^{57}Fe *h.f. anisotropy parameter for the* RFe_2 *series (in* kG). *At* 4.2 K A_{dip} *is computed for a saturated* R.E. *and for* $\mu_{Fe} = 1.6\ \mu_B$. *The variation of* μ_{Fe} *between* 4.2 *and* 295 K *is assumed to be proportional to that of the h.f. field in* $YbFe_2$.

	A_{dip} (0 K)	A (0 K)		A_{dip} (295 K)	A (295 K)	
$PrFe_2$	0.09	?		< 2 (a)	6 ?	(a)
$NdFe_2$	0.05	14 ± 1	(a, b)	< 1.3 (a)	11 ± 3	(a)
		14 ± 1 (field exp)	(a)		14 ± 2 (field exp)	(a)
$SmFe_2$	1.65	9.5 (4 K)	(c)	~ 2	10	(d)
		13 (80 K)	(c)			
$GdFe_2$	6.54	11.2 ? (77 K)	(e)			
$TbFe_2$	7.9	10.4 (77 K)	(f)			
		10.9 (4 K)	(c)			
		10.9 (80 K)	(c)			
$DyFe_2$	8.68	?		6.6 (g)	10 ?	(h)
$HoFe_2$	8.76	8.7	(i)	6 ? (h)	10 ?	(h)
$ErFe_2$	8.17	11.6 (4 K)	(c)		6.4 ?	(j)
		9 (80 K)	(c)			
$TmFe_2$	6.95	5.2 (80 K)	(c)	4.5 (l)		
		7 (77 K)	(k)			
$YbFe_2$	5	7.5 ± 2.5	(a)	2.5 (m)	12 ± 5	(a)
		~ 7 (field exp)	(a)		11.5 ± 2.5 (field exp)	(a)
$LuFe_2$	2.27	2	(n)	2.0	1	(n)

(a) This work.
(b) Ref. [4].
(c) BUSCHOW, *Rep. Prog. Phys.* **40** (1977) 1179, see p. 1245.
(d) VAN DIEPEN *et al.*, *Phys. Rev.* **B 8** (1973) 1125.
(e) $GdFe_2$ doped with 2 % Nd. Value measured on figure 1*a* of MIZOGUCHI *et al.*, *J. Physique Colloq.* **40** (1979) C2-211 (Mössbauer Conference, Kyoto).
(f) BOWDEN *et al.*, *J. Phys.* **C 2** (1968) 1376.
(g) Dy moment deduced from Mössbauer data of (f).
(h) Results of second order fits. BOWDEN, *J. Phys.* **F 3** (1973) 2206.
(i) $Ho_{0.8}Er_{0.2}Fe_2$. ATZMONY *et al.*, *Phys. Rev.* **B 7** (1973) 4220.
(j) Measured on spectra of Gubbens thesis (Delft 1977).
(k) WIESINGER, *J. Physique Colloq.* **37** (1976) C6-585 (Mössbauer Conference, Corfu).
(l) Tm moment deduced from M.E. : COHEN, *Phys. Rev.* **134 A** (1964) 94.
(m) Using M.E. data of [2, 3].
(n) GUIMARAES, A. P., Thesis, Manchester (1971). The uncertainty on these values is large (± 3).

When referred to the cubic axes, such a hamiltonian simulates dipolar effects. Indeed, in terms of $\mathcal{A}_{\parallel}^{hf}$ and $\mathcal{A}_{\perp}^{hf}$, the isotropic hyperfine field $\mathbf{H}_{iso}$ and the total anisotropy parameter A are given by [3],

$$\mathbf{H}_{iso} = \frac{\mathcal{A}_{\parallel}^{hf} + 2\,\mathcal{A}_{\perp}^{hf}}{3}\left|\frac{\boldsymbol{\mu}_{Fe}}{\mu_B}\right| + \\ + B[(g_J - 1)\,|\langle J_{R.E.}\rangle| \mp C\,|(2 - g_J)\langle J_{R.E.}\rangle|] \quad (14)$$

(in which the first term corresponds to $A'\langle S_{Fe}\rangle$ in equation (11)) and

$$A = A_{dip} + \frac{\mathcal{A}_{\parallel}^{hf} - \mathcal{A}_{\perp}^{hf}}{3}\left|\frac{\mu_{Fe}}{\mu_B}\right|. \quad (15)$$

In $NdFe_2$ at 0 K, $A_{dip} \simeq 0$, $H_n = 190$ kOe and $A = 14$ kOe.

Consequently it follows that,

$$\frac{\mathcal{A}_{\parallel}^{hf} - \mathcal{A}_{\perp}^{hf}}{(\mathcal{A}_{\parallel}^{hf} + 2\,\mathcal{A}_{\perp}^{hf})/3} \simeq \frac{H_{max}^{hf} - H_{min}^{hf}}{H_{iso}} \simeq \frac{3\,A}{H_n} \simeq 22\,\%. \quad (16)$$

While small compared to the effects observed for Fe^{++} ions (where $\mathcal{A}_{\parallel}$ can be $\sim 3\,\mathcal{A}_{\perp}$ [24]), such a h.f.s. anisotropy is appreciable for a metallic compound. As discussed in detail in reference [7], anomalies in the apparent dipolar field of probably the same origin have also been observed in other intermetallics such as Er_6Fe_{23} [25], $ErFe_3$ [26] and Tm_2Fe_{17} [27]. Moreover, important hyperfine anisotropies (up to 40 %) have been detected by N.M.R. in the Bloch walls of hexagonal YCo_5 and $SmCo_5$ [28, 29]. The authors attribute this Co h.f.s. anisotropy to a partially unquenched orbital moment on the cobalt

atom and correlate it with the high magnetocrystalline anisotropy of YCo_5 : $K_1 = 7.5 \times 10^7$ ergs/cm^3 at 24 K [30], as compared to cobalt metal : $K_1 = -0.79 \times 10^7$ ergs/cm^3 at 77 K [31].

Similarly, the cubic magnetocrystalline anisotropy ([4]) constant of YFe_2 : $K_1 \sim 1$ K per formula unit $\sim 3 \times 10^6$ ergs/cm^3 at 4.2 K [32] is appreciably higher than that of metallic Fe : $K_1 \sim 5 \times 10^5$ ergs/cm^3 at 77 K [31] which suggests that for the R.M. intermetallic compounds the d band is more polarizable than in the pure 3d metals, this being probably due to the addition of the 5d electrons of the rare earth. Such an increased polarizability would give, both a larger magnetocrystalline anisotropy of Co and Fe and an anisotropic contribution to their hyperfine structures.

Such an h.f.s. anisotropy, associated with the d band, is expected to vary smoothly across the RFe_2 series. In principle it should be given approximately by the value of $A - A_d$ in $LuFe_2$. However this quantity is not presently well known ([5]).

There might also exist a transferred contribution to the h.f.s. originating from the R.E. which in its simplest form could be written as follows,

$$\mathcal{H}^{hf}_{trans} = \sum_{i\ (R.E.)} \mathbf{I}.\mathfrak{B}_i.[b(g_J - 1) \mp c(2 - g_J)]\,\mathbf{J}_i \quad (17)$$

where $b(g_J - 1)\,\mathbf{J}$ and $c(2 - g_J)\,\mathbf{J}$ correspond respectively to the spin and orbital contributions. The corresponding effective hamiltonian would be the sum of two terms,

1) an isotropic part corresponding to the transferred contribution

$$B\,|\,(g_J - 1)\langle J\rangle\,| \mp |\,C(2 - g_J)\langle J\rangle\,|$$

as previously considered in § 6.3.1 (Eqs. (11, 14)) and 2) an anisotropic part corresponding to A :

$$\mathcal{H}^{an}_{trans} = \mathbf{I}.\mathfrak{B}''.|\,b(g_J - 1) \mp c(2 - g_J)\,|\,\langle \mathbf{J}\rangle \quad (18)$$

in which the traceless tensor $\mathfrak{B}''$ (proportional to A_d, Eq. (2')) would reflect the local trigonal symmetry at the iron. Such an effect might account for the apparently irregular behaviour of $A - A_d$ shown in table V. Note that more complicated anisotropic transferred contributions could also exist [23*b*].

([4]) The local second order spin hamiltonian DS_z^2 of the iron, if any, is a constant when summed over the four Fe sites, and the second order terms ($\sim D^2/\mu_B H_{ex}^{Fe\text{-}Fe}$) are expected to be small compared with the fourth order contribution :

$$a(S_x^4 + S_y^4 + S_z^4 + \cdots)$$

which gives rise to K_1. See [31], p. 182.

([5]) A seems to be small in $LuFe_2$ (Table V) but the behaviour of this compound is mainly determined by the impurities in the lutetium and the Mössbauer spectra cannot be unambiguously interpreted. A was also believed to be small in $GdFe_2$ until recent experiments with doped samples revealed a large A (Mizoguchi *et al.* [35]).

The transferred contribution of the Rare Earth, if any, should vary strongly with temperature, in contrast with effects associated with the d band anisotropy. Further studies of $A - A_d$ throughout the series, particularly as a function of temperature and in conjunction with R.E. Mössbauer experiments (which yield the R.E. moment), would be of interest for an improved understanding of these phenomena.

6.4 MAGNETIC HYPERFINE STRUCTURE AT THE RARE EARTH NUCLEUS. — As discussed in § 3.2 the hyperfine field at the Rare Earth nucleus is higher than the free ion hyperfine field in the second half of the series and lower in the first half (Table I). These deviations probably result from both self polarization effects and transferred fields from the iron.

Acknowledgments. — We are indebted to many people and it is a pleasure to thank them. The specimens were prepared with the help of Mr. M. Perroux using the high pressure apparatus of Dr. J. J. Capponi at the Laboratoire de Cristallographie. The magnetization measurements were performed with the help of Mr. J. L. Barlet in the Service Général de Mesures d'Aimantation of the Laboratoire Louis Néel. The high field experiments were made at S.N.C.I. and C.E.N.G. in collaboration with Dr. O. Massenet and Dr. J. Chappert. Finally, throughout this study we have benefited from very fruitful discussions with Dr. R. Lemaire and Dr. D. Givord.

APPENDIX

Dipolar effects in the RFe_2. — 1. COMPUTATION OF THE TOTAL DIPOLAR FIELD [33]. — To compute the total dipolar field at a point L (in practice an iron site) in an elliptical sample limited by a surface S_2 and having a volume magnetization $\mathbf{M}(\mathbf{r})$, as shown in figure 16, we draw around L a Lorentz sphere S_1 whose

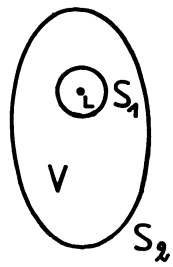

Fig. 16. — Ellipsoid showing the Lorentz sphere.

radius is large compared with the lattice spacing but small compared with the distance over which $\mathbf{M}(\mathbf{r})$ varies. The total dipolar field is then as follows,

$$\mathbf{H}^{tot}_{dip} = \mathbf{H}_{S_2} + \mathbf{H}_V + \mathbf{H}_{S_1} + \mathbf{H}_{dip} \quad (A.1)$$

$\mathbf{H}_{dip}$ is the field obtained by a point by point summation inside the Lorentz sphere. In the absence of h.f.s. anisotropy it is the same as the field $\mathbf{H}_d$ introduced in the main text (Eq. (2)), but otherwise is only one contribution (Eq. (15)).

$\mathbf{H}_{S_2}$ and $\mathbf{H}_{S_1}$ are the fields created by fictitious surface distributions of magnetic charge $\sigma = \mathbf{n}.\mathbf{M}(\mathbf{r})$ at each point of S_2 and S_1. $\mathbf{H}_V$ is the field created by a fictitious volume distribution of magnetization $\rho = -$ div $\mathbf{M}$ between S_1 and S_2. The conventional demagnetizing field is $\mathbf{H}_{S_2} + \mathbf{H}_V$.

In both a uniformly magnetized sample and in a sample with Bloch walls, div $\mathbf{M} = 0$, and therefore : $\mathbf{H}_V = 0$. On the other hand, since $\mathbf{M}$ is uniform over S_1, we have

$$\mathbf{H}_{S_1} = + \frac{4\pi}{3}\mathbf{M}_L \quad \text{(Lorentz field)}. \qquad (A.2)$$

As far as $\mathbf{H}_{S_2}$ is concerned, in a uniformly magnetized sample : $\mathbf{H}_{S_2} = -[N]\,\mathbf{M}$, ($[N]$ = demagnetizing tensor). However, for a domain structure in zero field where the average magnetization $\mathbf{M}$ is zero, $\mathbf{H}_{S_2} = 0$ except near the surface.

2. COMPUTATION OF THE TOTAL HYPERFINE FIELD AT THE IRON. — The relative orientations of the R.E. and iron moments $\boldsymbol{\mu}_{R.E.}$ and $\boldsymbol{\mu}_{Fe}$, of the resultant magnetization $\mathbf{M}$ and of the isotropic field at the iron $\mathbf{H}_{iso}$ (which is opposed to $\boldsymbol{\mu}_{Fe}$) are shown in figure 17*a* for the first half of the RFe_2 and in figure 17*b* and 17*c* for the second half of the series both below and above the compensation temperature.

A) *Total hyperfine field in a sample with Bloch walls in zero field* ($H_{S_2} = 0$, $H_V = 0$). — The total hyperfine field is given by,

$$\mathbf{H}_{tot} = \mathbf{H}_{iso} + \frac{4\pi}{3}\mathbf{M} + \mathbf{H}_d \equiv \mathbf{H}_n + \mathbf{H}_d \qquad (A.3)$$

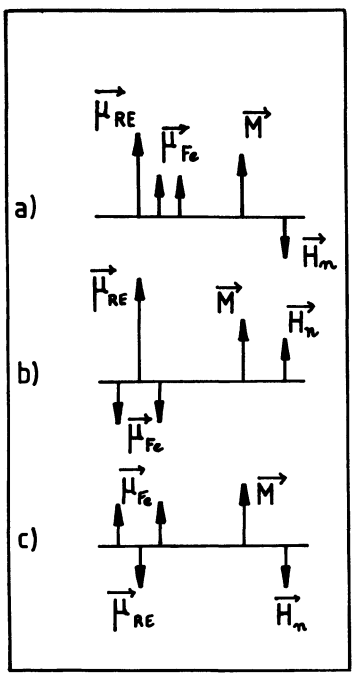

Fig. 17. — Relative orientation of the iron and R.E. moments $\boldsymbol{\mu}_{Fe}$ and $\boldsymbol{\mu}_{R.E.}$, of the resultant magnetization $\mathbf{M}$ and of the isotropic h.f. field $\mathbf{H}_n$ in the RFe_2 series : *a*) first half of the series ; *b*) second half of the series below T_{comp} ; *c*) second half of the series above T_{comp}.

in which $\mathbf{H}_{iso}$ is the « true » isotropic hyperfine field at the iron, $\frac{4\pi}{3}\mathbf{M}$ is the Lorentz field and $\mathbf{H}_n$ is the apparent isotropic field introduced in the main text, see § 2.3 ($\mathbf{H}_d$ is the anisotropic contribution, Eq. (2')). The relationship between H_n and H_{iso} varies throughout the series, as follows :

a) First half of the series,

$$|\mathbf{H}_n| = H_{iso} - \frac{4\pi}{3}M = H_{iso} + \frac{4\pi}{3v}[-2|\mu_{Fe}| - |\mu_{R.E.}|] \qquad (A.4)$$

(v being the volume per formula unit);

b) Second half of the series below T_{comp} :

$$|\mathbf{H}_n| = H_{iso} + \frac{4\pi}{3}M = H_{iso} + \frac{4\pi}{3v}[-2|\mu_{Fe}| + |\mu_{R.E.}|], \qquad (A.5)$$

c) Second half of the series above T_{comp} :

$$|\mathbf{H}_n| = H_{iso} - \frac{4\pi}{3}M = H_{iso} + \frac{4\pi}{3v}[-2|\mu_{Fe}| + |\mu_{R.E.}|]. \qquad (A.6)$$

According to equations (A.4), (A.5) and (A.6), the Lorentz contribution to $|\mathbf{H}_n|$ is :

$$\frac{4\pi}{3v}[-2|\mu_{Fe}| \mp |\mu_{R.E.}|] \qquad (A.7)$$

in which the iron term should be nearly constant across the series, while the R.E. term is not constant and changes sign in the middle of the series. This last contribution is not negligible. For saturated R.E. moments,

$$-\frac{4\pi}{3v}|\mu_{R.E.}| = -2.45\ \text{kG} \quad \text{for} \quad Nd^{3+}$$

$$+\frac{4\pi}{3v}|\mu_{R.E.}| = +7.96\ \text{kG} \quad \text{for} \quad Ho^{3+}.$$

This result is of importance because it has been [34] postulated that $\mathbf{H}_n$ contains a *transferred* contribution of the R.E., which is proportional to the R.E. spin (itself opposed to the iron spin) and is of the order 0-30 kG. However it should be a contribution to $\mathbf{H}_{iso}$:

$$\mathbf{H}_{iso} = A''\langle \mathbf{S}_{Fe}\rangle - B\langle \mathbf{S}_{R.E.}\rangle \qquad (A.8)$$

$$|H_{iso}| = A''\langle S_{Fe}\rangle + B|\langle S_{R.E.}\rangle| = A\langle S_{Fe}\rangle + B|(g_J - 1)\langle J_{R.E.}\rangle|. \qquad (A.9)$$

When this expression for H_{iso} is included in equations (A.4), (A.5) and (A.6) for $|H_n|$, they are replaced by :

$$|H_n| = A'\langle S_{Fe}\rangle + B|(g_J - 1)\langle J_{R.E.}\rangle| \mp \mp (4\pi\mu_B/3v)\, g_J\langle J_{R.E.}\rangle \qquad (A.10)$$

(with $A' = A'' - (16\,\pi\mu_B/3\,v)$), in which the two R.E. contributions are of comparable size.

It is this quantity which should be compared with experiment as is discussed in the main text (§ 6.3.1).

B) *Total hyperfine field in a pellet.* — We assume that the pellet shaped sample is submitted to an external field $\mathbf{H}_0$ perpendicular to the pellet and which is large enough to drive away the Bloch walls ($H_0 > 4\,\pi M$). The total field seen by the ^{57}Fe nucleus is :

$$\mathbf{H}_{tot} = \mathbf{H}_n \mp (\mathbf{H}_0 - 4\,\pi\overline{\mathbf{M}}) \qquad (A.11)$$

with a minus sign in cases *a*) and *c*)
a plus sign in case *b*).

$\overline{\mathbf{M}} = \mathbf{M}$ if the field is strong enough to rotate the domains and uniformly magnetize the sample (room temperature).

$|\overline{\mathbf{M}}| = M\cos\beta$ if the field only selects in each grain the nearest easy direction at an angle β from $\mathbf{H}_0$ (helium temperature).

References

[1] CANNON, J. F., ROBERTSON, D. L., HALL, H. T., *Mat. Res. Bull.* **7** (1972) 5.

[2] MEYER, C., SROUR, B., GROS, Y., HARTMANN-BOUTRON, F., CAPPONI, J. J., *J. Physique* **38** (1977) 1449.

[3] MEYER, C., GROS, Y., HARTMANN-BOUTRON, F., CAPPONI, J. J., *J. Physique* **40** (1979) 403 and Addendum : HARTMANN-BOUTRON, F., MEYER, C., *J. Physique* **41** (1980) 1075.

[4] MEYER, C., HARTMANN-BOUTRON, F., GROS, Y., SROUR, B., CAPPONI, J. J., *J. Physique Colloq.* **40** (1979) C5-191 (Physics of Metallic Rare Earths, Saint Pierre de Chartreuse, 1978).

[5] MEYER, C., HARTMANN-BOUTRON, F., GROS, Y., CAPPONI, J. J., *J. Physique Colloq.* **41** (1980) C1-191 (Mössbauer Conference, Portoroz 1979).

[6] MEYER, C., HARTMANN-BOUTRON, F., CAPPONI, J. J., CHAPPERT, J., MASSENET, O., *J. Magn. Magn. Mat.* **15-18** (1980) 1229 (ICM Munich 1979).

[7] MEYER, C., Thèse de Doctorat d'Etat, Grenoble (1980).

[8] SHIMOTOMAI, M., MIYAKE, H., DOYAMA, M., Submitted for publication.

[9] SHIMOTOMAI, M., MIYAKE, H., DOYAMA, M., *J. Phys. F*; *Metal Phys.* **10** (1980) 707.

[10] BUSCHOW, K. H. J., *Rep. Prog. Phys.* **40** (1977) 1179.

[11] *a*) DARIEL, M. P., ATZMONY, U., LEDENBAUM, D., *Phys. Status Solidi b* **59** (1973) 61.
b) ATZMONY, U., DARIEL, M. P., BAUMINGER, E. R., LEDENBAUM, D., NOWICK, I., OFER, S., *Proc. 10th Rare Earth Conference*, Carefree, Arizona (1973) p. 605.

[12] We are indebted to Dr. Francis HARTMANN for suggesting this method.

[13] ABRAGAM, A., BLEANEY, B., *Electron Paramagnetic Resonance of Transition Ions* (Clarendon Press Oxford) 1970, see p. 875.

[14] *a*) KOON, N. C., RHYNE, J. J., *Solid State Commun.* **26** (1978) 537.
b) RHYNE, J. J., KOON, N. C., *J. Appl. Phys.* **49** (1978) 2133.
c) RHYNE, J. J., KOON, N. C., ALPERIN, H. A. in *Rare Earths in Modern Science and Technology II*, edited by G. J. McCarthy, J. J. Rhyne, H. B. Silber (Plenum Press, N.Y.) 1980 ; See p. 133.

[15] FUESS, H., GIVORD, D., GREGORY, A. J., SCHWEIZER, J., *J. Appl. Phys.* **50** (1979) 200.

[16] BERTHIER, Y., DEVINE, R. A., BUTERA, R., to be published in *Proc. of Symposium on Nuclear and Electron Resonance Spectroscopies Applied to Materials Science*, Boston, Nov. 1980.

[17] WERTHEIM, G. K., JACCARINO, V., WERNICK, J. H., *Phys. Rev. A* **135** (1964) 151.

[18] GUIMARAES, A. P., Ph. D. Thesis, Manchester University (1971).

[19] ATZMONY, U., DARIEL, M. P., DUBLON, G., *Phys. Rev.* **B 14** (1976) 3713 ; *Phys. Rev.* **B 17** (1978) 396.

[20] ATZMONY, U., DUBLON, G., *J. Physique Colloq.* **37** (1976) C6-625 (Mössbauer Conference, Corfu 1976).

[21] *a*) WALLACE, W. E., SCRABEK, A. E., *Rare Earth Research* **2** (1964) 431 (Gordon and Breach, N.Y.) 1964.
b) BUSCHOW, K. H. J., VAN STAPELE, R. P., *J. Physique Colloq.* **32** (1971) C1-672 (I.C.M. Grenoble 1970).
c) GIVORD, D., GIVORD, F., LEMAIRE, R., *J. Physique Colloq.* **32** (1971) C1-668 (I.C.M. Grenoble 1970).
d) ILARRAZ, J., DEL MORAL, A., *Phys. Status Solidi a* **51** (1979) K 41.
e) BUSCHOW, K. H. J., *Rep. Prog. Phys.* **40** (1977) 1179.

[21 *bis*] See reference [7], p. 9. See also :
a) BUSCHOW, K. H. J., VAN STAPELE, R. P., *J. Appl. Phys.* **41** (1970) 4066.
b) BURZO, E., *Phys. Rev.* **B 6** (1972) 2882.
c) FISCHER, G., MEYER, A., *Solid State Commun.* **16** (1975) 355. A more elaborate treatment based on a band model can be found in :
d) CYROT, M., LAVAGNA, M., *J. Phys. F* (GB) **40** (1979) 763.

[22] VAN DIEPEN, A. M., DE WIJN, H. W., BUSCHOW, K. H. J., *Phys. Rev.* **B 8** (1973) 1125.

[23] *a*) BERTHIER, Y., DEVINE, R. A. B., BELORIZKY, E., *Phys. Rev.* **B 17** (1978) 4137.
b) BELORIZKY, E., NIEZ, J. J., BOUCHERLE, J. X., SCHWEIZER, J., LEVY, P. M., *J. Magn. Magn. Mat.* **15-18** (1980) 303 (ICM Munich 1979).

[24] HARTMANN-BOUTRON, F., IMBERT, P., *J. Appl. Phys.* **39** (1968) 775.

[25] GUBBENS, P. C. M., Ph. D. Thesis, Delft University Press (1977).

[26] VAN DER KRAAN, A. M., GUBBENS, P. C. M., BUSCHOW, K. H. J., *Phys. Status Solidi a* **31** (1975) 495.

[27] GUBBENS, P. C. M., BUSCHOW, K. H. J., *Phys. Status Solidi a* **34** (1976) 729.

[28] SEARLE, C. W., KUNKEL, H. P., KUPCA, S., MAARTENSE, I., *Phys. Rev.* **B 15** (1977) 3305.

[29] STREEVER, R. L., *Phys. Lett.* **65A** (1978) 360.

[30] HOFFER, G., STRNAT, K., *J. Appl. Phys.* **38** (1967) 1377.

[31] KANAMORI, J. in *Magnetism I*, edited by G. T. Rado and H. Suhl (Academic Press, N.Y.) 1963, p. 133.

[32] VAN DIEPEN, A. M., DE WIJN, H. W., BUSCHOW, K. H. J., *Proc. I.C.M.* (1973) Moscow, Vol. **I**, p. 227 (Publishing House Nauka, Moscow).

[33] HARTMANN-BOUTRON, F., Thèse, Paris (1963), Rapport C.E.A. R 2236 Saclay (1964).

[34] See reference [21*e*], p. 1217 and references therein.

[35] MIZOGUCHI, T., TANAKA, Y., TSUCHIDA, T., NAKAMURA, Y., *J. Physique Colloq.* **40** (1979) C2-211 (Mössbauer Conference Kyoto).